Analysis of Vehicle-Track Coupled Dynamics Model of Slab Ballastless Track Considering Cohesion Model

Zhicheng Liang, Kun Zhang* and Xinran Li

School of Civil Engineering, Dalian Jiaotong University, Dalian, Liaoning, China

*Corresponding author: zhk@djtu.edu.cn

Abstract. The debonding between CA mortar and track slabs has become a typical disease of ballastless tracks for high-speed railways. The interaction of track slab and CA mortar interface is relatively complex, and accurately simulating the bonding relationship between the two is very meaningful for the numerical analysis and damage detection of slab ballastless tracks. This article takes a typical vehicle and the ballastless track slab of CRTSII type as engineering backgrounds. By inserting cohesive elements into the interface of CA mortar and track slab to simulate their bonding effect, a numerical model of the vehicle and track is established by using finite element software. The vibration responses of the track and rails under vehicle load are obtained through coupled dynamic analysis, and the responses of typical measurement points from the track are selected as the verification parameter. It was verified that the model is reasonable by comparing its responses with existing relevant literature values. The research results indicate that the track displacement and acceleration vibration response obtained based on the established model meet the limit values and are close to the values in relevant literature. The slab ballastless track vehicle rail coupling dynamic model considering the cohesive force model can be used as the benchmark model for vehicle-track coupling dynamic analysis.

Keywords: Slab ballastless track; CA mortar; Debonding; Cohesive force element; Dynamic response

1 INTRODUCTION

Slab ballastless tracks are widely used and promoted for high-speed railways because of their advantages of simple structure, convenient construction, easy maintenance, low noise, smooth operation, and low operation and maintenance costs [1]. As an important infrastructure for high-speed railway transportation, ballastless track inevitably suffers from various diseases due to long-term exposure to the external environment, coupled with environmental factors and vehicle loads. Among these diseases, the cracking form of the debonding of mortar and track slab is to separate CA mortar from other parts of the structure (as shown in Figure 1), which is currently a prominent disease of track structures [2]. The debonding near CA mortar layer will reduce its binding force for the track plate, change the bearing ability and force

© The Author(s) 2024
B. Yuan et al. (eds.), *Proceedings of the 2024 8th International Conference on Civil Architecture and Structural Engineering (ICCASE 2024)*, Atlantis Highlights in Engineering 33,
https://doi.org/10.2991/978-94-6463-449-5_20

transmission path of the track structure, increase the deformation in warping of track plates or lead to fracture in mortar layer due to stress concentration. This will further seriously affect ballastless track the ride comfort, durability and driving comfort, and even for the safety of driving hidden dangers.

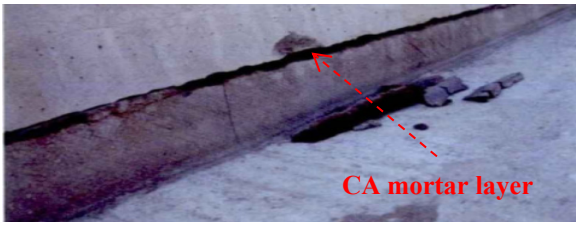

Fig. 1. CA mortar falls off and blocks fall off

Establishing a reasonable finite element numerical model for ballastless track is a prerequisite for analyzing ballastless track for the dynamic properties and detecting track defects from track dynamic characteristics. Interaction between CA mortar and track slab interface is quite complex. Accurately simulating the bonding relationship between the two is very important for dynamic analysis and disease detection for slab ballastless track. In the present research, there are two ways to simulate CA mortar layer. One is to set up spring element to simulate CA mortar between rail plate and support layer, and the other is to model the CA sand layer as a solid unit, and then simulate the interaction between CA mortar, track plate and support layer by contact or consolidation. However, in addition to bearing and transmitting vertical force in track system and attenuating vibration of the system, mortar layer acts as bonding to connect both the upper track plate and the underlying base plate as a whole, and transmit transverse and longitudinal forces to ensure the integrity of the whole track structure. Especially in the resistance to temperature, braking and other lateral or longitudinal load, the bond force from CA mortar plays an important role. However, it is usually difficult to accurately simulate the bonding force state of CA mortar surface. In addition, ballastless track structure, as a long and large reinforced concrete structure, works in complex environment for many years. The debonding damage of CA mortar in it always starts from the temperature load which changes repeatedly. After the interlaminar damage occurs under the temperature gradient load, the interlaminar bond weakens or fails, at this point, the interaction between the temperature load and the train dynamic load has a strong nonlinear interaction, which will lead to the problems such as CA mortar layer dropping, rail slab arching, and so on [3]. These diseases will affect the track irregularity, and then affect the increase of vehicle load on the track dynamic role. And so, it is meaningful to establish a finite element numerical model for the multi-factor coupling analysis of track dynamic characteristics.

The essence of CA mortar debonding of ballastless track is the crack between mortar and adjacent components. Cohesion model, as a model for simulating crack initiation and propagation based on elastoplastic fracture mechanics, has been widely used in the deformation and damage analysis for ballastless track structure under temperature effect in recent years[3-5]. These studies proved that the insertion of cohesion

elements below track slab and above mortar layer can well simulate the track deformation with temperature change. This also provides an alternative choice for the finite element analysis facing ballastless track under the coupling action of vertical vehicle load and horizontal load. As far as we know, establishing a finite element numerical model for track structure considering cohesive elements with ANSYS software and using it to study dynamic characteristics of track under vehicle load has not been carried out. Based on this, this paper takes a typical vehicle and the ballastless track slab of CRTSII type as engineering backgrounds, a numerical model of train-track is established by inserting a cohesive element below track plate and above mortar layer with ANSYS software, the ballastless track vehicle-track coupling dynamic model is proved to be reasonable by coupling and dynamic analysis.

2 BASIC THEORY FOR COHESION MODEL

Cohesion theory was developed from Hillerborg's Fictitious Crack Model in 1976. The original virtual fracture model was only suitable for the simulation of tensile fracture, but later scholars improved the existing cohesive fracture model, referred to as Cohesive Zone Model. After this model is improved, it has been paid much attentions in civil engineering materials, composite materials interface cracking, bond structure cracking and other issues, and can realize a good description of interface damage law and its failure mechanism in the concrete. The idea of the cohesion model is to describe the crack propagation by using the constitutive relation of the cohesion t and the opening displacement δ, and to simulate the mechanical behaviors for the crack interface materials by choosing appropriate parameters. Here, the cohesion element Inter205 (in Figure 2) is inserted below track slab and above mortar layer to simulate their interaction. The relation law of tension and displacement of the common cohesion model is mainly in the form of bilinear and exponential. The researches show that the linear cohesion model fits for brittle fracture, whereas the exponential cohesion model can used in the case of elastic-plastic fracture with large amplitude or totally plastic deformation [6-7]. The cracking above mortar layer and below track slab is brittle cracking. Therefore, this article uses a bilinear tension displacement relationship to simulate it, as shown in Figure 3.

Because the actual cracks on both sides of CA mortar are tension cracks, a tension crack is the dominant mode in this paper, the correlation between the normal force and its corresponding displacement is expressed as

$$T_n = K_n \delta_n (1 - D_n) \tag{1}$$

$$K_n = \frac{T_n^{max}}{\delta_n^*} \tag{2}$$

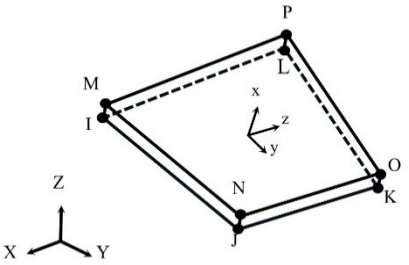

Fig. 2. INTER205 element diagram

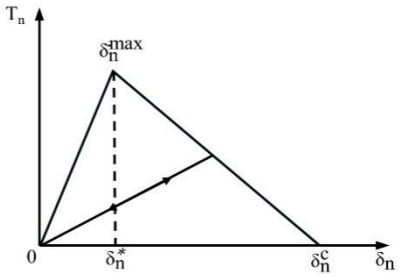

Fig. 3. Bilinear tension-displacement curve

where T_n and T_n^{max} represents normal cohesion and maximum normal cohesion, respectively. δ_n and δ_n^* respectively represent normal displacement and its value when the traction force reaches the maximum normal cohesion, δ_n^c is the normal displacement when debonding is completed, and K_n is normal cohesion stiffness.

Tangential forces and displacements are assumed to follow the same law as normal forces and displacements as

$$T_t = K_t \delta_t (1 - D_n) \tag{3}$$

$$K_t = \frac{T_t^{max}}{\delta_t^*} \tag{4}$$

The meaning of each element is similar to the above and will not be repeated. When setting the parameters, set the maximum tangential cohesion to a negative number. In both cases, the damage parameter D_n is defined as

$$D_n = \begin{cases} 0 & \delta_n^{max} \le \delta_n^* \\ \left(\frac{\delta_n^{max} - \delta_n^*}{\delta_n^{max}}\right)\left(\frac{\delta_n^c}{\delta_n^c - \delta_n^*}\right) & \delta_n^* < \delta_n^{max} \le \delta_n^c \\ 1 & \delta_n^{max} > \delta_n^c \end{cases} \tag{5}$$

where δ_n^{max} is the maximum displacement in the separation process, when the displacement between the two structures is greater than the displacement when the

debonding is completed, it means that the two structures have been completely separated and there is no force between them.

3 ESTABLISHMENT OF COUPLED MODEL FOR VEHICLE AND TRACK CONSIDERING COHESIVE MODEL

3.1 Finite Element Numerical Model of Track

Ballastless track with CRTSII slab is a type of modern railway tracks independently developed in our country, which has good adaptability and is extensively applied to construct modern railway in our country. The dimensions and components of track with CRTSII slabs are illustrated in Figure 4. The whole system is composed of supporting layer, CA mortar, track slab, fastener and rail from bottom to top.

Because the beam-body finite element model is based on material and geometric parameters of the components most closely to ballastless tracks, it has mostly potential to accurately simulate the components and their connection, therefore, a beam-body numerical model is used to model CRTSII slab track in this study. The rail of CHN60 is simulated with BEAM188 element, which allows the user to customize the beam cross-section to meet the requirement of establishing the irregular cross-section. The fastener system is simulated using a linear spring element of type COMBINE14, which mainly provides the vertical force and the longitudinal sliding resistance for the rail, and each node of the unit has three degrees of freedom, it has longitudinal or torsional function in one-dimensional, two-dimensional or 3D, and can simulate the deformation and force of fastener well. The stiffness of spring is 6.0×10^7, and the damping is 4.77×10^4. The Solid65, a commonly used solid element with eight nodes and three degrees of freedom on each node, is used in simulating track slab, mortar and supporting layer because it can also simulate the forces and deformations of three kinds of structures. The detailed parameters of the main components in track structure are valued according to reference[8] and are shown in Table 1.

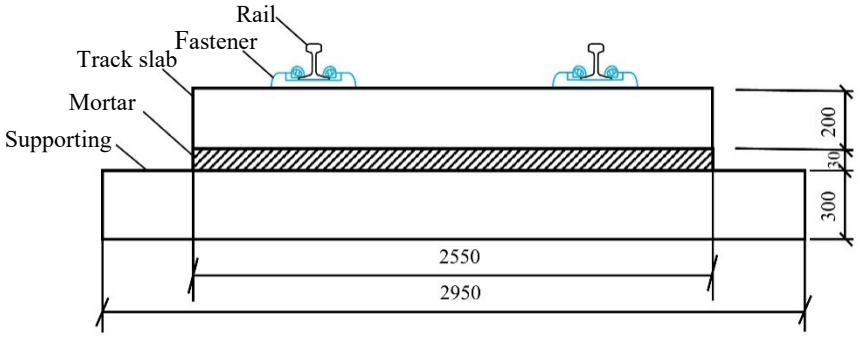

Fig. 4. Diagram of track with CRTSII slab

Table 1. Parameters and their values of track with CRTSII slab

Members	Young's modulus (MPa)	Poisson's ratio	Density ($kg \cdot m^{-3}$)	Linear expansion coefficient (m/℃)
Rail	2.06×10^5	0.30	7800	1.2×10^{-5}
Track slab	3.6×10^4	0.17	2500	1.18×10^{-5}
Mortar	8.0×10^3	0.34	2400	1.3×10^{-5}
Supporting	3.0×10^4	0.20	2500	1.0×10^{-5}

In addition, this model simulates the bonding below track slabs and above mortar by inserting a cohesive element between them. The constitutive relation in cohesion model is introduced into the cohesion element by defining material properties and setting real constants, according to the measurement values of specimens in tensile and shear strength tests made by the authors of reference [9] , Table 2 lists the selected concrete real constants of the cohesion model. Figure 5 gives an end view of the finite element numerical model of track with CRTSII slab including cohesion element.

Table 2. Parameters and their values in cohesion model

Parameters	Meanings	Properties	Values
C1	σ_{max}	Normal maximum cohesion (N)	7906
C2	δ_n^c	Normal displacement with debonding completed (mm)	0.99×10^{-3}
C3	T_{max}	Tangential maximum cohesion (N)	-5780
C4	δ_t^c	Tangential displacement when debonding is completed (mm)	0.7874
C5	α	δ_n^*/δ_n^c or δ_t^*/δ_t^c	0.878

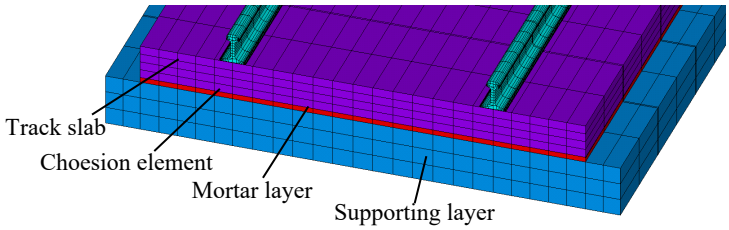

Fig. 5. End view of CRTSII slab track finite element model including cohesion element

3.2 Vehicle-track Coupled Dynamics Model

The coupled model of vehicle and track considering vehicle and track as an whole coupled interactive system, and the vehicle and track are coupled through the interface of wheel and rail. The sub-model representing vehicle and a wheel-rail interface relationship are as shown in Figure 6.

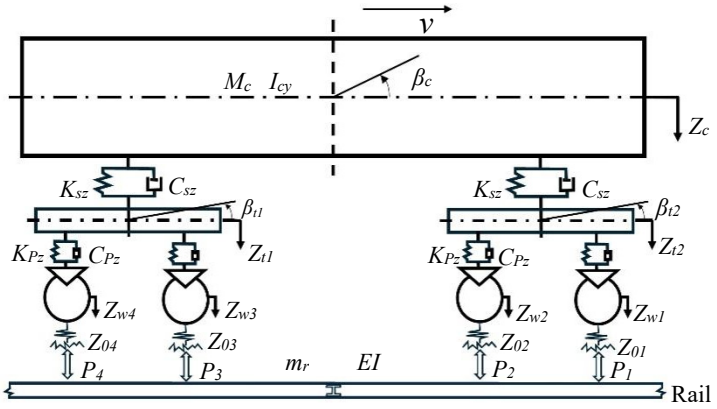

Fig. 6. The vehicle dynamics model

The vehicle model consists of two sets of spring-damping system. A single car is composed of a car body, a front bogy, a rear bogy and four wheelsets. Considering the body and the bogie before and after the head and the up-and-down movement and the up-and-down movement of four wheelsets, it totally has 10 freedom degrees. COMBINE14, a spring element, is adopted to numerically represent the primary suspension and secondary suspension systems. Whereas bogies, wheelsets and car body are simplified as particles and simulated with Mass21. The whole vehicle model adopts the form of 1-motor + 2-trailer, and the specific dynamic parameters for vehicle are listed in Table 3 [10].

Table 3. Values of parameters for high-speed vehicle model

Parameter Names	Moving cars	Trailer
Car body mass (kg)	59364.219	40000
Frame mass (kg)	5630.851	2100
Wheelset mass (kg)	1843.52	1950
Car body nodding inertia (kg·m^2)	1723415.315	2560000
Frame nodding inertia (kg·m^2)	9487.860	2100
Stiffness for primary suspension (N·m^{-1})	2.3996×10^6	0.6×10^6
Damping for primary suspension (N·s·m^{-1})	3×10^4	1×10^4
Stiffness for secondary suspension (N·m^{-1})	0.8858×10^6	0.26×10^6
Damping for secondary suspension (N·s·m^{-1})	4.5×10^4	6×10^4

4 VALIDATION OF DYNAMICS MODEL OF VEHICLE AND TRACK

Taking track irregularity as excitation source [10], and taking it as a periodic sine function with wavelength of 12.5 m and amplitude of 3 mm, dynamic responses both from vehicle and track are calculated when the high-speed vehicle (1 moving + 2 towing) passes through three track slabs (19.29 m) at 200 km/h in speed. Both dis-

placements and accelerations of the intermediate nodes from rail and track slab in the midpoint section are shown in figures 7 to 10.

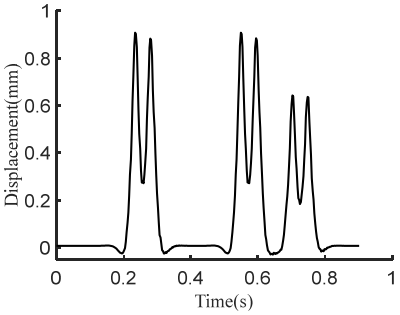

Fig. 7. Vertical disp. from rail midpoint

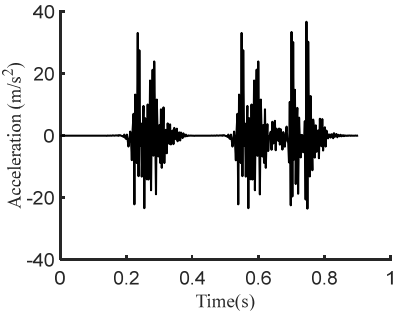

Fig. 8. Vertical acc. from rail midpoint

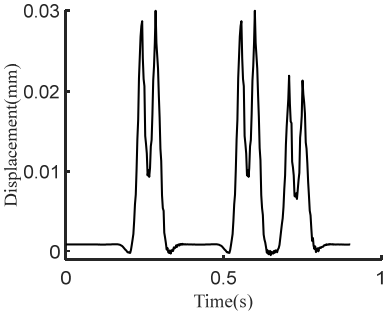

Fig. 9. Vertical disp. from track slab midpoint

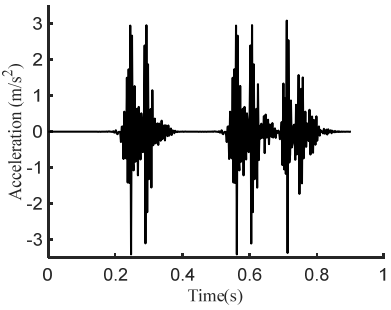

Fig. 10. Vertical acc. from track slab midpoint

In order to prove the model validity, Table 4 compares the above calculation results of the established model with those of reference [10].

Table 4. Amplitudes of vertical responses from this model and the model in reference [10]

Calculation items	This model	Model in Ref.[10]
Rail midpoint disp./mm	0.908	0.778
Rail midpoint acc./(m·s^{-2})	36.822	31.265
Track slab midpoint disp./mm	0.030	0.024
Track slab midpoint acc./(m·s^{-2})	3.413	3.012

As can be seen from the results in figures 7-10 and table 4, the values of the calculated values for each part of the track using the established cohesive vehicle-track coupling dynamic model are all within the normal range, the dynamic amplitudes in two results all basically conform to the change law, which presents both validity and feasibility of the numerical model established in this paper. It can basically presents major dynamic characteristics of CRTSII slab ballastless track and vehicle coupling system.

5 CONCLUSION

Based on CRTSII slab ballastless track and typical EMU, a numerical model of coupling vehicle and track is firstly founded with ANSYS software in simulating the bond between slab and CA mortar by using cohesion model. The responses of ballastless tracks under dynamic vehicle load are obtained by coupling dynamic analysis with track irregularity as excitation source. The established numerical model of vehicle and track is verified to be reasonable by comparing responses of the typical measuring points obtained from the model with the relevant literature values. These results show the established dynamic model for vehicle-track of slab ballastless track considering cohesion model can describe the bonding effect below slab and above mortar in ballastless track with CRTSII slab more closely. It provides a more accurate and reli-

able basic numerical model of vehicle-track for studying track dynamic characteristics under multi-direction and complex loads such as temperature and vehicle. The model can be used as a basic model for the future research on the disease of ballastless tracks, especially for diagnosing diseases about track CA mortar void.

ACKNOWLEDGMENTS

Authors wishing to acknowledge supports in funds from the Research Foundation from Chinese Natural Science Foundation with Grant No. of 51978127 and College Students Innovation Program from Dalian Jiaotong University with Grant No. of 202310150326.

REFERENCES

1. Esveld C. (2003) Developments in High-Speed Track Design. In: Transportation-IABSE Symposium. Antwerp. pp. 27-29. https://www.doi.org/10.2749/222137803796328782
2. Hu Q. and Shen Y. (2023) CA mortar void identification for slab track utilizing time-domain markov chain monte carlo-based bayesian approach. Structural Health Monitoring, 22 (6):3971-3984. https://www.doi.org/10.1177/14759217231166117
3. Jin Z. (2020) Dynamic Influence and Identification of Mortar GAP Damage of CRTS II Slab Ballastless Track in High Speed Railway, Southwest Jiaotong University, Chengdu. https://www.cnki.net
4. Hu S., Zhou X., Xu. Q, Zhou S. (2019) The study of interface damage extension between CRTS Ⅱ slab and CA mortar under temperature gradient. Journal of Railway Science and Engineering,16(9):2143-2149. https://www.doi.org/10.19713/j.cnki.4-1423/u.2019.09.002
5. Du W., Ren J., Du J. and Qu C. (2024) Influence of interlayer adhesion parameters on interface damage of prefabricated slab track. Journal Huazhong University of Science & Technology (Natural Science Edition),52(2):210-126. https://www.doi.org/10.13245/j.hust.240759
6. Yamakov V., Saether E., Phillips D. R. and Glaessgen E. H. (2006) Molecular-dynamics simulation-based cohesive zone representation of intergranular fracture processes in aluminum. Journal of the Mechanics and Physics of Solids, 54(9):1899-1928. https://www.doi.org/10.1016/j.jmps.2006.03.004
7. Wang X. (2014) Calculation of the Gap between CRSTII Slab and Mortar and Analysis on its Influence Characteristic of Track Dynamics. Central South University, Changcha. https://www.cnki.net
8. Xu Y., Yan D., Zhu W. and Zhou Y. (2020) Study on the mechanical performance and interface damage of CRTS II slab track with debonding repairment. Construction and Building Materials, 257:119600. https://www.doi.org/10.1016/j.conbuildmat.2020.119600
9. Li P. (2017) Analysis of the Interface Damage of CRST II Slab Track and its Influnces. Southwest Jiaotong University, Chengdu. https://www.cnki.net
10. Chen X. (2005) Rail Engineering. China Construction Industry Press, Beijing. http://www.sslibrary.com/

Open Access This chapter is licensed under the terms of the Creative Commons Attribution-NonCommercial 4.0 International License (http://creativecommons.org/licenses/by-nc/4.0/), which permits any noncommercial use, sharing, adaptation, distribution and reproduction in any medium or format, as long as you give appropriate credit to the original author(s) and the source, provide a link to the Creative Commons license and indicate if changes were made.

The images or other third party material in this chapter are included in the chapter's Creative Commons license, unless indicated otherwise in a credit line to the material. If material is not included in the chapter's Creative Commons license and your intended use is not permitted by statutory regulation or exceeds the permitted use, you will need to obtain permission directly from the copyright holder.